J. Biochem. **136**, 635–641 (2004)
DOI: 10.1093/jb/mvh171

Nickel-Binding Properties of the C-Terminal Tail Peptide of *Bacillus pasteurii* UreE

Hyung-Sik Won* **and Bong-Jin Lee†**

National Research Laboratory (MPS), Research Institute of Pharmaceutical Sciences, College of Pharmacy, Seoul National University, San 56-1, Shillim-Dong, Kwanak-Gu, Seoul 151-742, South Korea

Received July 25, 2004; accepted August 19, 2004

Urease activation, which is critical to the virulence of many human and animal pathogens, is mediated by several accessory proteins. UreE, the only nickel-binding protein among the urease accessory proteins, catalyzes the activation of urease by transporting nickel ions into the urease active sites. The nickel-binding properties of UreE are still not clear, particularly for the protein from *Bacillus pasteurii* (Bp). Since the flexible C-terminal tail of BpUreE possesses two conserved histidines, the nickel-binding properties of the tail peptide were examined by circular dichroism spectroscopy, size-exclusion chromatography, and nuclear magnetic resonance spectroscopy. Specific nickel binding leading to alteration of the peptide backbone geometry was clearly observed. Side-chains of the two conserved histidines were identified as the main ligands for nickel coordination. The peptide became dimerized upon nickel binding and the binding stoichiometry was estimated as 1 equivalent of nickel per peptide dimer. Altogether, it is postulated that the C-terminal tail of BpUreE contributes to the nickel binding of the protein in different ways between the dimeric and tetrameric protein folds.

Key words: *Bacillus pasteurii*, C-termianl tail peptide, nickel binding, urease, UreE.

Urease is a nickel-containing enzyme that catalyzes the hydrolysis of urea to produce ammonia and carbamate (*1*, *2*). Increased pH arising from this reaction is critical to the virulence of several human and animal pathogens (*1*, *3*). Thus, the molecular details of the urease-related biological systems are a matter of primary concern for many scientists, who are attempting to provide targets for potential drugs able to abolish the negative effects of bacterial urease activity (*4*, *5*). Urease possesses multiple active sites containing nickel ions, and the proper assembly of this metallocenter is a key step in urease activation. Among the urease accessory proteins, including UreD, UreE, UreF, UreG, and UreH, that are required for urease maturation (*6–9*), UreE is a metallochaperone that delivers nickel ions into the urease active sites (*2*, *10*, *11*).

All the UreE proteins possess conserved histidines to bind nickel ions, and many UreE proteins from various species possess His-rich C-terminal tails (*12–14*). The number of histidines conserved in the C-terminal tail differs among species, and their functional role is still unclear. The UreE protein from *Klebsiella aerogenes* (Ka), which possess 10 histidines in the last 15 residues, provides an example of a multi-His–containing tail. In contrast, the *Bacillus pasteurii* (Bp) UreE C-terminal tail has only two conserved histidines, and thus represents a tail with only a few histidines. Most of the nickel-binding properties of UreE have been investigated for KaUreE, while less is known about the nickel-binding properties of BpUreE.

The KaUreE dimer binds up to six nickel ions, while the H144*UreE dimer, a truncated form lacking 15 residues from the C-terminus, can bind only two or three nickel ions (*14–16*). The crystal structure of the mutant (H91A or H110A substitution) H144*UreE showed three copper ions bound to the protein dimer (*17*). Therefore, the C-terminal tail of the KaUreE dimer is responsible for the independent nickel binding of up to three equivalents. In the case of BpUreE, it has also been proved that the protein, at a physiological (micromolar) concentration, behaves as a dimer, both in the presence and absence of metal ion (*5*, *13*). However, paramagnetic NMR investigation at high (millimolar) protein concentration indicated a binding stoichiometry of 0.25 equivalents of nickel per subunit. Subsequently, it was revealed that the protein, at millimolar concentrations, becomes tetramerized upon the binding of a metal ion, such as zinc or nickel (*13*). Finally, the zinc-bound BpUreE (Fig. 1), which was crystallized at a millimolar concentration, shows two forms of tetrameric folds sharing one zinc ion on the dimer-dimer interface (*10*). In this crystal structure, the C-terminal tail was found as a long coil and the C-terminal conserved residues (-G144-H145-Q146-H147) were not visible in the electron-density map, probably due to the highly flexible nature of the region.

In summary, the nickel-binding properties of the BpUreE C-terminal tail have never been elucidated. Due to the limitations in the BpUreE crystal structures, it is still not clear whether the C-terminal tail of BpUreE contributes to the nickel binding of the protein in the dimeric and/or tetrameric state. The disordered, flexible nature of

*Current address: Department of Molecular Biology, The Scripps Research Institute, 10550 North Torrey Pines Road, La Jolla, CA 92037, USA.
†To whom correspondence should be addressed. Fax: +82-2-872-3632, E-mail: lbj@nmr.snu.ac.kr

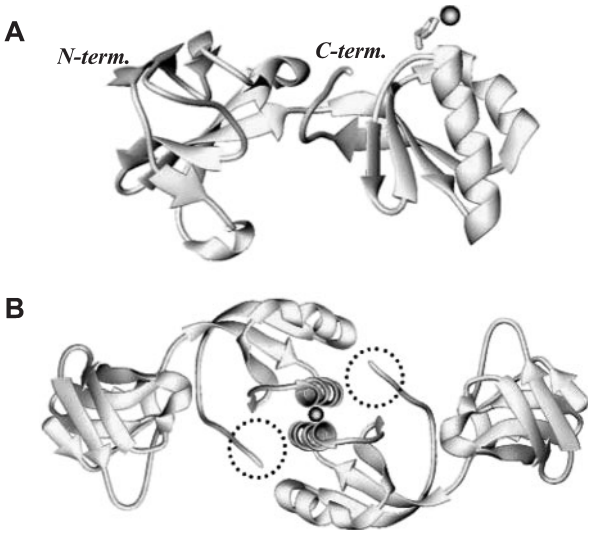

Fig. 1. **Ribbon presentation of the zinc-bound BpUreE structure.** The bound zinc ion is represented as a gray sphere. A: Front view of the BpUreE monomer unit. The His 100 side chain is shown as a ball and stick model. B: Top view of the dimeric unit in the BpUreE tetramer structure. The flexible C-terminal tail regions are indicated by dotted circles. The metal-binding site constitutes the dimer-dimer interface in the tetrameric structure. These drawings were produced with the UCSF MidasPlus program using the coordinates for the zinc-bound BpUreE crystal structure (PDB accession code 1EB0). The last four residues (-G144-H145-Q146-H147) are not visible from these coordinates.

the C-terminal tail makes it reasonable to study a synthetic peptide corresponding to the region. Thus, in the present study, we examined the nickel-binding properties of the synthetic BpUreE C-terminal tail peptide, by circular dichroism (CD) and nuclear magnetic resonance (NMR) spectroscopy, and by size-exclusion chromatography. The results comprise the first structural data demonstrating the nickel-binding properties of the BpUreE C-terminal tail.

MATERIALS AND METHODS

Peptide Sample Preparation—All of the sample peptides, including BpUreECt (N-acetyl-KEPFKYRGHQH-COOH; m.w. 1,468), a synthetic peptide corresponding to the C-terminal 11 residues of BpUreE, were purchased from ANYGEN (Kwang-ju, Korea; URL, http://www.anygen.com) as HPLC-purified freeze-dried powder. The sequence and purity of the peptides were confirmed by mass spectrometry and HPLC. Samples for spectroscopic and chromatographic experiments were prepared by dissolving the precise amount of peptide powder in 20 mM sodium phosphate buffer (pH 6.5) containing 150 mM NaCl. Sample pH was finely adjusted by the addition of 0.1 N HCl or NaOH. Nickel ions were added from a stock solution of $NiCl_2$ in pure water.

CD Spectroscopy—CD spectra were obtained at 298 K on a JASCO J-720 spectropolarimeter using a 0.1 cm pathlength cell with a 1 nm bandwidth, a 4 s response time, a scan speed of 50 nm/min, and a 0.2 nm step resolution. At every measurement, three individual scans were added and averaged, and the solvent CD signal was subtracted. CD scans of 0.6 mM and 2 mM BpUreECt were taken from 300 nm to 190 nm, with increasing concentrations of nickel. At each nickel addition, 2 μl of $NiCl_2$ stock solution was added into the 1 ml peptide solution.

Size-exclusion Chromatography—A Phenomenex BioSep-SEC-S2000 column connected to a Hitachi LC-organizer equipped with L-4200H UV-VIS Detector, L-6200 Intelligent Pump, and D-2500 Chromato-Integrator was used for the size-exclusion chromatography. The column was equilibrated with a mobile-phase solution: 20 mM sodium phosphate buffer containing 100 mM NaCl or 1.2 mM $NiCl_2$ at pH 6.5. Aliquots of 20–25 μl of a solution containing 0.5–1.0 mg/ml sample were injected onto the column, and the sample was eluted with the same mobile phase at a flow rate of 1 ml/min. During the elution, the absorbance at 214 nm was measured continuously and plotted versus time. Two peptides were used as molecular size references: a 23-residue peptide (NH_2-GILDTLKQ-FAKGVGKDLVKGAAQ-COOH; m.w. 2,358) that corresponds to the N-terminal 23 residues of an antimicrobial peptide gaegurin 4 (*18*, *19*), and a 13-residue peptide (NH_2-LGALFKVASKVLP-COOH; m.w. 1,343) that corresponds to residues 2–14 of an antimicrobial peptide gaegurin 5 (*20*, *21*).

NMR Spectroscopy—1D ^{1}H-NMR spectra of 4 mM BpUreECt were measured on a Bruker DRX 500 spectrometer at 308 K. The solvent water signal was suppressed by applying a pulsed-field gradient. Non-labile proton signals were discriminated by D_2O exchange experiments with the same spectra measured immediately after the addition of deuterated solvent to a sample lyophilized from non-deuterated solvent. All spectra were processed using X-Win NMR software.

RESULTS

Peptide Selection—In the crystal structure of BpUreE (Fig. 1), the residues from Y129 to R134 make up the last secondary structure element of the protein, and the next 9 residues are found as an unstructured coil conformation (*10*). The final four residues (-G144-H145-Q146-H147) are not visible in the crystal structure, probably due to the highly flexible nature of the region. Additionally, the backbone NMR chemical shifts of the last 11 residues in BpUreE are characteristic of a random-coil conformation (*22*, *23*). Thus, in this work, we used a synthetic peptide, BpUreECt, which corresponds to the C-terminal 11 residues (K137 to H147) of the protein, in order to investigate the nickel-binding properties of the flexible C-terminal tail of BpUreE. The N-terminus of the peptide was acetylated to mimic a continuous peptide bond. In the present work, the flexible, disordered conformation of the BpUreECt peptide was confirmed by CD and NMR spectroscopy (refer to the following subsections).

As molecular size references for the size-exclusion chromatography of BpUreECt, two inactive fragments of antimicrobial peptides were chosen for the following reasons (*18–21*). The peptide sizes of the 23-residue reference and the 13-residue reference are close to those of the dimeric and the monomeric BpUreECt, respectively. The two reference peptides commonly have neither histidine residues nor biological activity. In aqueous solution, both

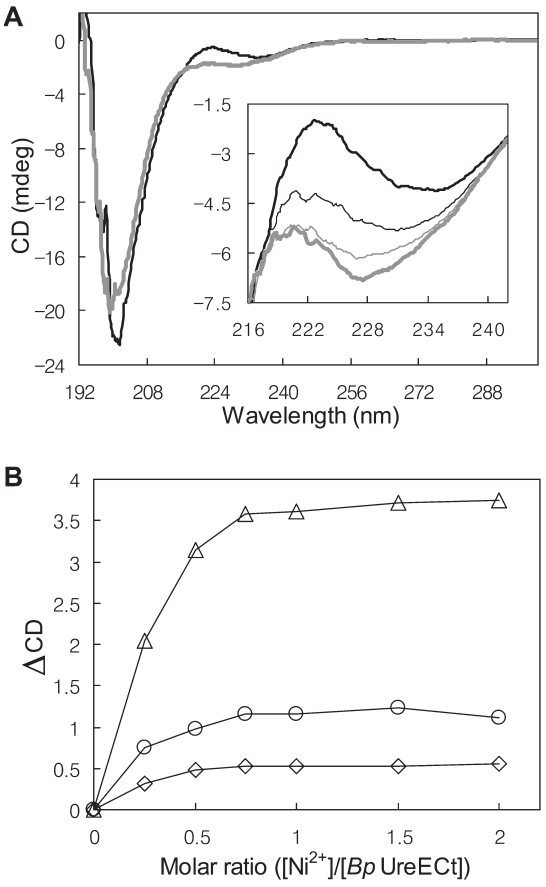

Fig. 2. **CD results demonstrating nickel binding to BpUreECt.** A: CD spectra of 0.6 mM BpUreECt in the absence of nickel (black) and in the presence of 1.2 mM $NiCl_2$ (gray). In the inset, the CD spectra of 2 mM BpUreECt, in the presence of 0 (bold black), 0.25 (thin black), 0.5 (thin gray), and 2 (bold gray) equimolar $NiCl_2$, are shown from 216 to 242 nm. B: $\Delta\theta_{227}$ (triangle), $\Delta\theta_{235}$ (circle) and $\Delta[\theta_{227}/\theta_{235}]$ (diamond) are plotted as a function of nickel concentration. The peptide concentration was 2 mM.

peptides are as highly soluble as BpUreECt and show no evidence of oligomerization. Both peptides in aqueous solution adopt a mainly random-coil conformation.

CD Spectroscopy—Far-UV CD signals are dominated by the peptide backbone geometry (*24*). As shown in Fig. 2A, CD spectra of BpUreECt in the absence of nickel show two distinct negative bands in the far-UV region. The strong, negative band centered near 200 nm, together with the weak, negative band at 235 nm, are typically indicative of a random-coil conformation (*25*). Upon the addition of nickel ions, the strong band near 200 nm was weakened, while the weak band at 235 nm intensified with a shift toward 227 nm. This changing pattern implies that the flexible random-coil portion in the peptide structure was decreased, and instead a small portion with a rather rigid or ordered structure was formed. Thus, the CD change upon the addition of nickel indicates an acquired conformational restraint on the peptide, probably by specific nickel binding. Although all of the nickel-induced signal changes were qualitatively reproducible, the change in the region below 210 nm was not quantitatively reproducible due to instrumental limitations (low signal-to-noise ratio below 210 nm). Thus, the weak band near 230 nm was subjected to a quantitative recording of spectral change. For this nickel titration, a high (2 mM) concentration of peptide was employed to intensify the weak, broad band around 230 nm. Since the center of the band shifted from 235 nm in the absence of nickel to 227 nm in the presence in nickel ion, the CD changes at 227 nm ($\Delta\theta_{227}$) and 235 nm ($\Delta\theta_{235}$), and the change of their ratio ($\Delta[\theta_{227}/\theta_{235}]$) were monitored and plotted in Fig. 2B as a function of the added nickel concentration. The nickel-induced spectral change was nearly complete, even with a half equivalent of nickel per peptide; *i.e.*, quite more than half of the binding sites in the 2 mM peptides were saturated by 1 mM nickel ions. This means that the binding stoichiometry should be less than 1 and around 0.5 equivalents of nickel per peptide, which can be achieved when at least two peptide molecules share one nickel ion. Thus, nickel-induced oligomerization of the peptide was expected to yield the small binding stoichiometry value of less than 1. To confirm the nickel-induced oligomeric state of BpUreECt, size-exclusion chromatography was performed.

Size-Exclusion Chromatography (Fig. 3)—First, in the absence of nickel in the mobile-phase buffer containing 100 mM NaCl salt, we confirmed that the BpUreECt peptide does not oligomerize. BpUreECt exhibited a retention time of 12.45 min (Fig. 3E), which is in agreement with the retention time of the 13-residue size-marker peptide (12.34 min; Fig. 3D) rather than the 23-residue size-marker peptide (11.18 min; Fig. 3C). When a BpUreECt solution containing 1 mM nickel ions was injected, the retention time decreased moderately (12.01 min; Fig. 3F). The decrease in retention time was not so large as to reflect an oligomeric behavior, and it could also not be attributable to a conformational change, since the CD (Fig. 2) and NMR (Fig. 4) results indicated little change in the overall conformation upon nickel binding. Thus, it could be supposed that the BpUreECt peptide initially (before being injected) in the nickel-containing solution had adopted a molecular system larger than a monomer, and then dissociated into monomers upon dilution into the nickel-free solution (mobile-phase buffer) while migrating in the column. This also suggests that the nickel-binding affinity would be so low that the bound nickel was gradually released during migration. Thus, to detect clearly the nickel-bound state of BpUreE, 1 mM nickel ions were added to the mobile-phase buffer. In addition, to enhance the nickel-binding affinity of the peptide and to increase the resolution of the elution profiles, additional salt was excluded from the mobile-phase buffer. Under these conditions, we could rule out the possibility of unfavorable adsorption on the column resin or undesirable aggregation of the samples, since all of the samples were well-eluted with expected peak volumes, favorable peak shapes, and reproducible retention times. In this environment, the elution profile of the nickel-containing BpUreECt solution showed two distinct peaks, one at 13.14 min and the other at 17.22 min (Fig. 3L). The former peak, with a retention time close to that of the 23-residue reference (Fig. 3I), and the latter, of which retention time is close to that of the 13-residue reference (Fig. 3J), could be assigned to the dimeric and the monomeric forms of BpUreECt, respectively. These assign-

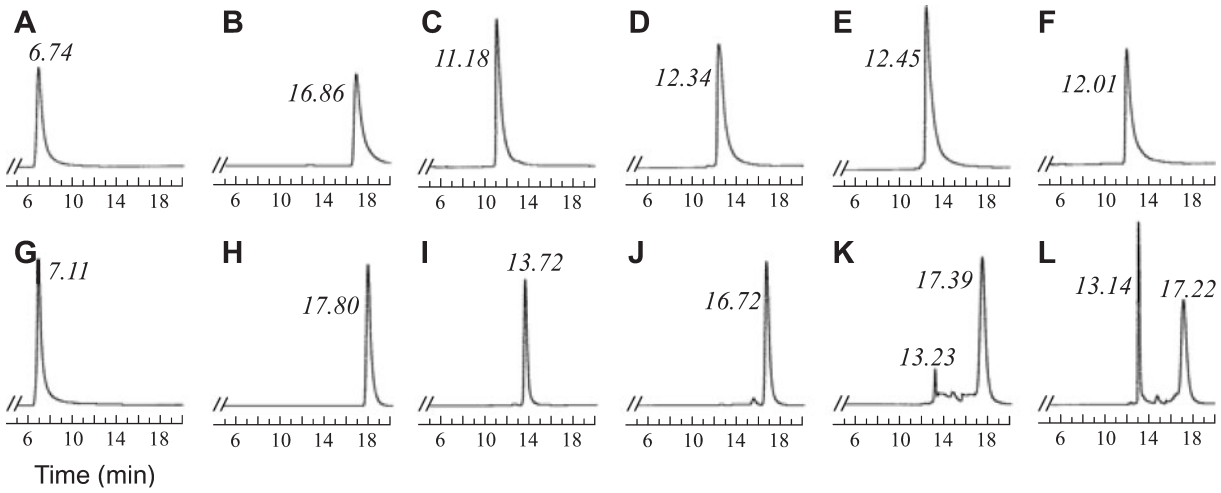

Fig. 3. **Size-exclusion chromatography of BpUreECt.** 20 mM sodium phosphate buffer (pH 6.5) containing 100 mM NaCl (A–F) or 1 mM $NiCl_2$ (G–L) was used as the mobile phase. Elution peaks are labeled with their retention times. Injected samples were: (A and G) Blue-dextran (m.w. 2,000,000), (B and H) Tryptophan (m.w. 204), (C and I) 23-residues size-marker peptide (m.w. 1,343), (D and J) 13-residues size-marker peptide (m.w. 2,358), (E and K) BpUreECt (m.w. 1,468) without Ni^{2+}, and (F and L) BpUreECt solution containing 1 mM $NiCl_2$. Blue Dextran and Tryptophan were used to estimate the column void volume and the total bed volume, respectively.

ments were supported by the fact that the amount of the former peak was severely reduced, while the latter peak intensified in the elution profile of the nickel-free BpUreECt solution (Fig. 3K). Both peaks showed more increased retention times in the elution profile of the nickel-free BpUreECt solution (13.23 and 17.39 min; Fig. 3K) than in the profile of the nickel-containing BpUreECt solution (13.14 and 17.22 min; Fig. 3L). This also implies that the molecular size of the injected BpUreECt was larger in the nickel-containing solution than in the nickel-free solution, although there was re-equilibration of the two forms (monomer and dimer) during the elution process allowing dilution, probably due to the low affinity. In addition, the BpUreECt dimer peak was very sharp relative to other peptide peaks, including the peak of the monomeric BpUreECt, suggesting that the peptide acquired a conformational restraint, probably by nickel binding. When the mobile-phase buffer contained addi-

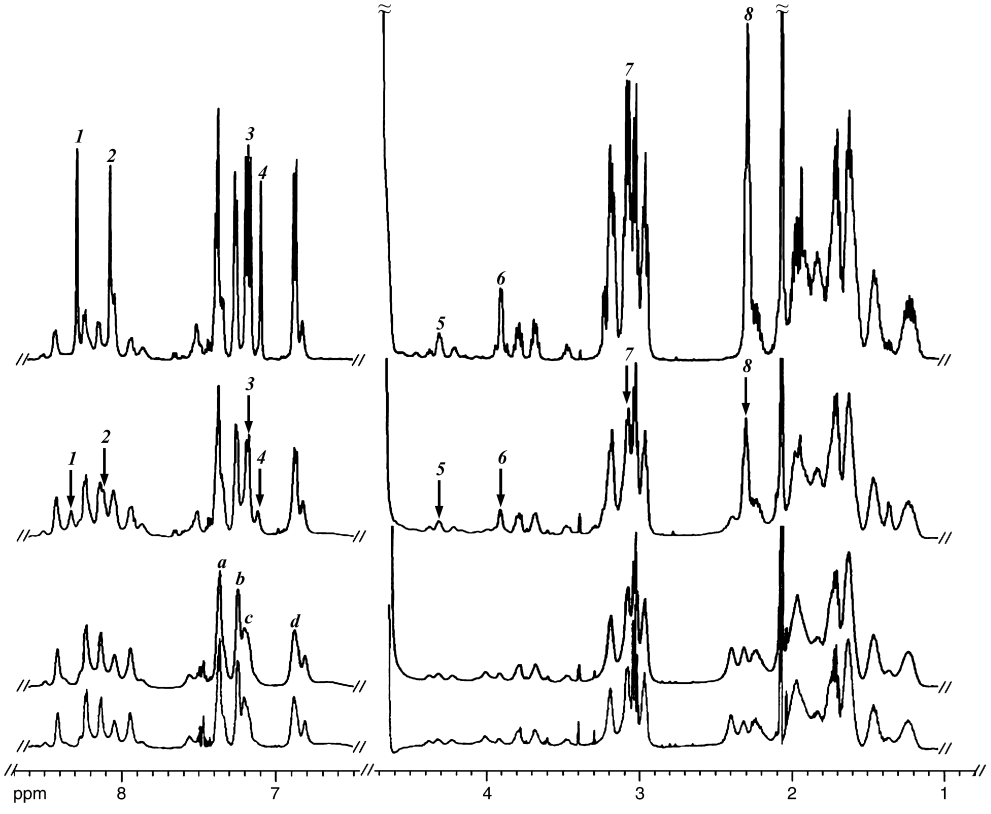

Fig. 4. **1D ^{1}H-NMR spectra of BpUreECt (*N*-acetyl-KEPFKYRGHQH-COOH) in the presence of 0, 0.3, 0.5, and 1.0 equivalent of nickel ion (upper to bottom).** The two strongest peaks, including the solvent signal, were removed from for clarity all spectra (indicated by ≈). Representative resonances that reasonably show specific broadening upon nickel binding are indicated by numbers from 1 to 8. The resonances from the aromatic ring protons are represented by letters (a–d)

tional salt (100 mM NaCl), no peak assignable to the dimeric BpUreECt could be observed, but the retention time of BpUreECt was always decreased by the addition of nickel into the mobile-phase buffer or injected solution (data not shown). Taken together, the size-exclusion results of BpUreECt indicate that the nickel-bound state of BpUreECt is a dimer, although the nickel-binding affinity is rather low.

NMR Spectroscopy—NMR spectra were employed to identify the ligand residues for the specific nickel binding of BpUreECt (Fig. 4). Consistent with the CD spectra, the NMR spectra of BpUreECt support a disordered conformation of the peptide by showing a narrow dispersion of backbone amide proton resonances. Upon increasing the nickel concentration, no overall perturbation in the chemical shifts was observed, but an overall line-broadening occurred in the spectra. This means that the overall conformational change was small, but the rotational correlation time of the peptide was increased, probably due to an enlarged molecular system, such as a dimeric conformation. In addition to the overall line-broadening, more significant broadening was observed for several specific resonances. In particular, peaks 1–8 in Fig. 4 were almost completely broadened, probably due to the paramagnetic effect of the bound nickel ion, while most of the other resonances remained without any specific broadening. Among the resonances that disappeared upon nickel binding, the intense resonances in the amide region (peaks 1 and 2) could be assigned to side-chain protons rather than backbone amide protons for their remarkable intensity. They were confirmed to be non-labile resonances, since they were not exchanged by solvent deuterium (data not shown). Finally, supported by their chemical shifts at 8.06 and 8.28 ppm, peaks 1 and 2 could be unambiguously assigned to the ε1 protons of His residues. For the same reason, it was reasonable to assign the non-labile resonances 3 and 4 to the δ2 protons of His residues. Thus, the results indicate that both of the His residues in BpUreECt are specifically involved in the nickel binding. In contrast, no specific broadening was observed for the other non-labile resonances in the amide region (peaks a–d), which could be assigned to aromatic ring protons. This means that the Phe and Tyr residues in BpUreECt do not contribute to the nickel binding of the peptide. In addition, most of the amide proton resonances remained without specific change. In summary, the NMR results lead to the conclusion that the histidine side-chains in BpUreECt mainly contribute to the nickel binding of the peptide.

As judged from the NMR spectra (Fig. 4), significant portion of the nickel-binding sites were not filled by 0.33 equivalents of nickel, whereas nickel binding was almost saturated with 0.50 equivalents of nickel. For the NMR experiments, the peptide concentration was so high (4 mM) that it probably allowed most of the added nickel to be bound. Thus, the results indicate that the nickel-binding stoichiometry of BpUreECt is higher than 0.33 and near 0.5 equivalents per peptide. Thus, considering all of the present CD, NMR, size-exclusion results together, the nickel-binding stoichiometry of BpUreECt should be between 0.33 and 1.0 (most probably, 0.5) nickel per peptide and its nickel-bound state should be an oligomer (most probably, a dimer). Finally, we conclude that BpUreECt becomes dimerized upon nickel binding, and that the specific nickel-binding stoichiometry is one nickel ion per dimer.

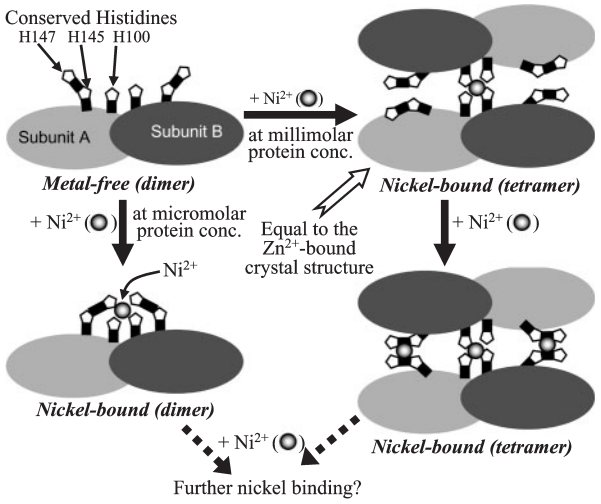

Fig. 5. **Schematic model illustrating the suggested nickel-binding mode of BpUreE.** In this model, the C-terminal tails are involved in the nickel binding of the protein at both micromolar and millimolar concentrations, but in different ways (refer to the text for detailed description).

DISCUSSION

Conserved histidines in UreE proteins are located at two different sites, at the core and in the C-terminal tail (*12–14*). BpUreE possesses three conserved histidines, one at the core (His 100) and two in the C-terminal tail (His 145 and His 147). In particular, the last four residues (-G144-H145-Q146-H147) of BpUreE is a conserved sequence in many UreE proteins. Despite the detailed information from the crystal structure of the zinc-bound BpUreE, the nickel-binding properties of the C-terminal tail have not been defined. From the present investigation on the BpUreE C-terminal tail peptide, it is clear that the C-terminal tail sequence of BpUreE possesses an inherent ability to bind nickel, coordinated mainly by His side-chains, by adapting a dimeric conformation. As judged by size-exclusion chromatography, the nickel binding seems to be rather weak at the peptide level. However, the nickel binding would be stabilized if close proximity between two peptide molecules was ensured, as in the tetrameric structure of BpUreE (*10*). In the tetrameric folds of BpUreE, two C-terminal tails in a dimeric unit are proximately faced on the tails of the opposite dimeric unit. Thus, additional metal binding would be plausible at the interfaces between the tails (Fig. 5), which would not be seen in the crystal structure. Subsequently, our laboratory has confirmed that the tetrameric fold of BpUreE can bind more than one (at least three) nickel ions, and, particularly, the C-terminal tail is responsible mainly for the additional nickels above 1 equivalent (*22*). It is still not clear whether the tetrameric folds of the protein are physiologically relevant (*5*, *10*, *13*). Apparently, the tetrameric structure of BpUreE is not expected to be formed under physiological conditions, since an unusually high

protein concentration is required in vitro for the protein to tetramerize. However, since the apo-urease complex possesses multiple active sites where nickel ions are delivered by UreE protein (*3*, *4*), the local concentration of BpUreE in vivo might be raised dramatically in its functional state where nickel transports from the protein to urease occur frequently. If this is the real case, then BpUreE would adopt a tetramer to put multiple nickel ions into a nearby nickel-binding site where an interaction with urease can occur. For this, as illustrated in Fig. 5, the C-terminal tail should play an important role in the additional nickel trapping.

In the known structure of the zinc-bound BpUreE tetramer, the bound metal ion is coordinated by four histidines: two H100 residues from each dimeric unit (*10*). Thus, it can be postulated that two histidines would be insufficient for nickel binding in the dimeric state of BpUreE, which is physiologically relevant. The present results indicate that the histidines in the C-terminal tail can serve as ligands for nickel binding. Based on the crystal structure, the C-terminal tails of BpUreE in a dimeric fold are located proximately toward the H100 residues that serve as the main ligands for the metal binding (Fig. 1). Thus, the present results suggest that the C-terminal histidines in the dimeric fold of BpUreE could act as alternative ligands of histidines from another dimeric unit (Fig. 5). Subsequently, the data suggest that the C-terminal histidines of the dimeric BpUreE are indeed involved in its nickel binding, together with the H100 residues (*22*). This suggestion indicates a difference between BpUreE and KaUreE. In the case of the KaUreE dimer (*14–17*), 10 conserved histidines in the C-terminal tail can independently bind several nickel ions, and are not responsible for the nickel binding at the protein core. In addition, the present results, which indicate an inherent nickel-binding ability of the C-terminal tail, also suggest that even the dimeric fold might be able to bind more than 1 nickel ion. Finally, our progressing data have revealed that the dimeric BpUreE can bind approximately 3 equivalents of nickel ions at its maximum (*22*).

In conclusion, the present study on the BpUreE C-terminal tail peptide indicates for the first time that the nickel-binding ability of the C-terminal tail region is significant for the nickel-binding function of the protein, no matter which conformation, dimer, tetramer, or both, is assumed for the functional state of the protein. Finally, subsequent investigations on the nickel-binding properties of the whole BpUreE protein (*22*) can be encouraged and interpreted based on the present results.

This work was supported by the National Research Laboratory Program (M1-0203-00-0075) from the Korea Institute of Science & Technology Evaluation and Planning, Republic of Korea, by the Korea Science & Engineering Foundation (2000-2-20900-010-3, R01-2000-00144), and in part by the 2002 BK21 project for Medicine, Dentistry, and Pharmacy.

REFERENCES

1. Mobley, H.L.T. and Hausinger R.P. (1989) Microbial ureases: significance, regulation, and molecular characterization. *Microbiol. Rev.* **53**, 85–108
2. Lee, M.-H., Pankratz, H.S., Wang, S., Scott, R.A., Finnegan, M.G., Johnson, M.K., Ippolito, J.A., Christianson, D.W., and Hausinger, R.P. (1993) Purification and characterization of *Klebsiella aerogenes* UreE protein: a nickel-binding protein that functions in urease metallocenter assembly. *Protein Sci.* **2**, 1042–1052
3. Benini, S., Rypniewski, W.R., Wilson, D.S., Miletti, S., Ciurli, S., and Mangani, S. (1999) A new proposal for urease mechanism based on the crystal structures of the native and inhibited enzyme from *Bacillus pasteurii*: why urea hydrolysis costs two nickels. *Structure Fold. Des.* **7**, 205–216
4. Ha, N.-C., Oh, S.-T., Sung, J.-Y., Cha, K.-A., Lee, M.-H., and Oh, B.-H. (2001) Supramolecular assembly and acid resistance of *Helicobacter pylori* urease. *Nat. Struct. Biol.* **8**, 505–509
5. Lee, Y.-H., Won, H.-S., Lee, M.-H., and Lee, B.-J. (2002) Effects of salt and nickel ion on the conformational stability of *Bacillus pasteurii* UreE. *FEBS Lett.* **522**, 135–140
6. Park, I.-S. and Hausinger, R.P. (1995) Evidence for the presence of urease apoprotein complexes containing UreD, UreF, and UreG in cells that are competent for in vivo enzyme activation. *J. Bacteriol.* **177**, 1947–1951
7. Soriano, A., Colpas, G.J., and Hausinger, R.P. (2000) UreE stimulation of GTP-dependent urease activation in the UreD-UreF-UreG-urease apoprotein complex. *Biochemistry* **39**, 12435–12440
8. Sebbane, F., Mandrand-Berthelot, M.-A., and Simonet, M. (2002) Genes encoding specific nickel transport systems flank the chromosomal urease locus of pathogenic yersiniae. *J. Bacteriol.* **184**, 5706–5713
9. O'Halloran, T.V. and Culotta, V.C. (2000) Metallochaperones, an intracellular shuttle service for metal ions. *J. Biol. Chem.* **275**, 25057–25060
10. Remaut, H., Safarov, N., Ciurli, S., and Beeumen, J.V. (2001) Structural basis for Ni^{2+} transport and assembly of the urease active site by the metallochaperone UreE from *Bacillus pasteurii*. *J. Biol. Chem.* **276**, 49365–49370
11. Colpas, G.J. and Hausinger, R.P. (2000) In vivo and in vitro kinetics of metal transfer by the *Klebsiella aerogenes* urease nickel metallochaperone, UreE. *J. Biol. Chem.* **275**, 10731–10737
12. You, J.-H., Song, B.-H., Kim, J.-G., Lee, M.-H., and Kim, S.-D. (1995) Genetic organization and nucleotide sequencing of the ure gene cluster in *Bacillus pasteurii*. *Mol. Cells* **5**, 359–369
13. Ciurli, S., Safarov, N., Miletti, S., Dikiy, A., Christensen, S.K., Kornetzky, K., Bryant, D.A., Vandenberghe, I., Devreese, B., Samyn, B., Remaut, H., and Van Beeumen, J. (2002) Molecular characterization of *Bacillus pasteurii* UreE, a metal-binding chaperone for the assembly of the urease active site. *J. Biol. Inorg. Chem.* **7**, 623–631
14. Colpas, G.J., Brayman, T.G., Ming, L.-J., and Hausinger, R.P. (1999) Identification of metal-binding residues in the *Klebsiella aerogene*s urease nickel metallochaperone, UreE. *Biochemistry* **38**, 4078–4088
15. Brayman, T.G. and Hausinger, R.P. (1996) Purification, characterization, and functional analysis of a truncated *Klebsiella aerogenes* UreE urease accessory protein lacking the histidine-rich carboxyl terminus. *J. Bacteriol.* **178**, 5410–5416
16. Colpas, G.J., Brayman, T.G., ; Mccracken, J., Pressler, M.A., Babcock, G.T., Ming, L.-J., Colangelo, C.M., Scott, R.A., and Hausinger, R.P. (1998) Spectroscopic characterization of metal binding by *Klebsiella aerogenes* UreE urease accessory protein. *J. Biol. Inorg. Chem.* **3**, 150–160
17. Song, H.K., Mulrooney, S.B., Huber, R., and Hausinger, R.P. (2001) Crystal structure of *Klebsiella aerogenes* UreE, a nickel-binding metallochaperone for urease activation. *J. Biol. Chem.* **276**, 49359–49364
18. Won, H.-S., Park, S.-H., Kim, H.E., Hyun, B., Kim, M., Lee, B.J., and Lee, B.-J. (2002) Effects of a tryptophanyl substitution on the structure and antimicrobial activity of C-terminally truncated gaegurin 4. *Eur. J. Biochem.* **269**, 4367–4374
19. Park, S.-H., Kim, Y.-K., Park, J.-W., Lee, B., and Lee, B.-J. (2000) Solution structure of the antimicrobial peptide gaegurin 4 by ^{1}H and ^{15}N nuclear magnetic resonance spectroscopy. *Eur. J. Biochem.* **267**, 2695–2704

20. Park, S.-H., Kim, H.E., Kim, C.-M., Yun, H.-J., Choi, E.-C., and Lee, B.-J. (2002) Role of proline, cysteine and a disulphide bridge in the structure and activity of the anti-microbial peptide gaegurin 5. *Biochem. J.* **368**, 171–182
21. Won, H.-S., Jung, S.-J, Kim, H.E, Seo, M.-D., and Lee, B.-J. (2004) Systematic peptide engineering and structural characterization to search for the shortest antimicrobial peptide analogue of gaegurin 5. *J. Biol. Chem.* **279**, 14784–14791
22. Won, H.-S., Lee, Y.-H., Kim, J.-H., Shin, I.S., Lee, M.H., and Lee, B.-J. (2004) Structural characterization of the nickel-binding properties of *Bacillus pasteurii* urease accessory protein (Ure)E in solution. *J. Biol. Chem.* **279**, 17466–17472
23. Lee, Y.-H., Won, H.-S., Ahn, H.-C., Park, S., Yagi, H., Akutsu, H., and Lee, B.-J. (2002) Backbone NMR assignments of the metal-free UreE from *Bacillus pasteurii*. *J. Biomol. NMR* **24**, 361–362
24. Purdie, N. and Brittain, H.G. (1994) *Analytical Applications of Circular Dichroism*, Elsevier, Amsterdam
25. Rodger, A. and Nordén, B. (1997) *Circular Dichroism and Linear Dichroism*, Oxford University Press, Oxford